PCCP

Accepted Manuscript

ROYAL SOCIETY OF CHEMISTRY

www.rsc.org/pccp

PCCP

ARTICLE

Tip-enhanced Raman spectroscopy of bradykinin and its B_2 receptor antagonists onto colloidal suspended Ag nanowires

Received 00th June 2015,
Accepted 00th xxxx 2015

DOI: 10.1039/x0xx00000x

www.rsc.org/

D. Święch,[a] I. Tanabe,[b] S. Vantasin,[b] D. Sobolewski,[c] Y. Ozaki,[b] A. Prahl,[c] S. Maćkowski,[d] and E. Proniewicz*[a]

The tip-enhanced Raman scattering (TERS) spectra of bradykinin (BK) and its potent B_2 BK receptor antagonists, [D-Arg^0,Hyp^3,Thi^{5,8},L-Pip^7]BK] and [D-Arg^0,Hyp^3,Thi^5,D-Phe^7,L-Pip^8]BK, approximately with the size about 40 nm, were recorded onto colloidal suspended Ag nanowires with diameter in the range of 350 – 500 nm and length of 2 – 50 μm. The metal surface plasmon resonance and morphology of the Ag nanowires were studied by ultraviolet-visible (UV-Vis) spectroscopy and scanning electron microscope (SEM). Briefly, it was shown that two *C*-terminal amino acids of BK and [D-Arg^0,Hyp^3,Thi^{5,8},L-Pip^7]BK] are involved in the interaction with the colloidal susupended Ag nanowire surface, whereas three last amino acids of the [D-Arg^0,Hyp^3,Thi^5,D-Phe^7,L-Pip^8]BK sequence attached the Ag surface. Thus, BK adorbs on the colloidal susupended Ag nanowires mainly through the Phe$^{5/8}$ ring (tilted orientation) and the one oxygen atom of the carboxylate group and the Arg^9 H_2N–C–NH–CH_2– fragment of Arg^9. In case of [D-Arg^0,Hyp^3,Thi^{5,8},L-Pip^7]BK], the Thi^8 ring (through the lone electron pair on the sulfur atom) and the both oxygen atoms of the carboxylate group and the amine group of Arg^9 mainly participated in the interaction with the Ag nanowire surface. For [D-Arg^0,Hyp^3,Thi^5,D-Phe^7,L-Pip^8]BK, the D-Phe^7 ring, Pip^8 ring, and Arg^9 side-chain assisted in the peptide interaction with the Ag surface. The obtained results emphasize the importance of the *C*-terminal part of these peptides in the adsorption process onto the colloidal suspended Ag nanowires.

Introduction

The combination of Raman spectroscopy (RS) and scanning probe microscopy (SPM) results in a unique technique known as tip-enhanced Raman spectroscopy (TERS), developed at the beginning of this century.[1-3] The uniqueness of TERS is due to the advantages of the component techniques, such as: the chemical and structural sensitivity and the nanometer scale spatial resolution beyond the diffraction limit of light provided by RS and SPM, respectively.[1-5]

In TERS, a very sharp bulk metal or metal-coated tip (usually with a tip radius less than 50 nm) is brought into feedback with the sample using atomic force microscope (AFM) or scanning tunneling microscope (STM) setup.[6,7] Through illuminating the tip, being in a close proximity to the sample, by a focused laser beam the lightening rod effect, the optical nanoantenna effect, and the localized surface plasmons (LSP) excitation of a metallic surface occur that provide a strongly enhanced field at the apex of the probing tip.[8-10] The mechanism of the signal enhancement in TERS is generally the same as that in surface-enhanced Raman scattering (SERS) and can be explained mainly by classical electromagnetic (EM) and less often by chemical (CM) mechanisms.[8-11] The magnitude of the Raman signal enhancement for molecules in the close vicinity to the sharp tip, that is similar or greater than that in SERS (typically up to 10^9 or more), is very often discussed on the basis of SERS.[12-14] However, the surface enhancement effect in TERS strongly depends not only on the orientation of the electric field along the tip axis but also on the dimension of the tip end; thus, the spatial resolution is determined by the size and shape of the tip apex.[13,14] Because of it the accessible spatial resolution is typically less than 100 nm.[15,16] Tips are usually made of Ag and Au and are either etched from a metal wire or metal is deposited onto a standard AFM cantilever. Another, more elaborate probes are in the form of metal tips with bow-tie end structures or with special periodic structures for effective excitation and focusing of surface plasmon polaritons.

TERS is used for samples in air,[12] vacuum,[17] and solution[18]. It was successfully applied as a sensing instrument in studies of variety of carbon based molecules.[19,20] Although there is only a limited number of the TERS investigations on cell membranes,[21] nucleic acids,[22,23] viruses and bacteria,[24,25] lipids and human cell,[26] proteins, peptides, and amino acids[27-29].

In our laboratory, we also developed TERS for micro-topographic, high-resolution, and high-sensitivity detection of biologically active molecules in order to understand environmental and structural factors that may help to clarify the biological

[a] *Faculty of Foundry Engineering, AGH University of Science and Technology, ul. Reymonta 23, 30-059 Kraków, Poland. Email: proniewi@agh.edu.pl*
[b] *Department of Chemistry, School of Science and Technology, Kwansei Gakuin University, Gakuen 2-1, Sanda, Hyogo 669-1337, Japan.*
[c] *Faculty of Chemistry, University of Gdansk, Wita Stwosza 63 , 80– 308 Gdansk, Poland.*
[d] *Institute of Physics, Faculty of Physics, Astronomy, and Informatics, Nicolaus Copernicus University, Grudziadzka 5, 87– 100 Torun, Poland, and Wrocław Research Center EIT+, Stablowicka 147, Wroclaw, Poland.*
† Electronic Supplementary Information (ESI) available: See
DOI: 10.1039/x0xx00000x

behavior observed for these molecules. Recently, we have reported the TERS results for bradykinin (BK; Arg[1]-Pro[2]-Pro[3]-Gly[4]-Phe[5]-Ser[6]-Pro[7]-Phe[8]-Arg[9]COOH (all amino acids are in the *L*-conformation)) immobilized onto the colloidal suspended Ag nanoparticles.[30] These results have demonstrated that the bands of the same peptide fragments approximately having the same orientations with respect the colloidal suspended Ag film, with randomly distributed different-sized aggregates (high up to ~50 nm, length 80 – 500 nm) of the 20 nm spherical Ag nanoparticles, arise from the different probing points onto the Ag film. Some changes in these bands relative intensities among the TERS spectra recorded at the different probing points have been attributed to the heterogeneity of the colloidal suspended Ag surface than to molecules adsorbed on "hot spots".

In the present paper, we applied TERS to determine adsorption mode of native BK and its potent B_2 BK receptor antagonists: [D-Arg[0],Hyp[3],Thi[5,8],L-Pip[7]]BK and [D-Arg[0],Hyp[3],Thi[5],D-Phe[7],L-Pip[8]]BK (where: Hyp denotes to *L*-hydroxyproline, Thi – *L*- thienylalanine (tiophene), and Pip – *L*-pipecolic acid) (Table 1 presents the amino acid sequence of the investigated peptides) deposited onto colloidal suspended Ag nanowires. The choice of the colloidal suspended Ag nanowires as biosensor was due to the fact of it easy preparation, reproducibility, and long-term stability. Also, because it is clear that the rheology of adsorbed species, at monolayer and submonolayer coverage, onto a metallic surface and the strength of competitive interaction of certain molecular fragments with this surface depend on molecule structure and nanostructure of a metallic surface, and hence on controlled distribution of the metal surface plasmon. This is why it is necessary to investigate the TERS effect for molecules` at different experimental and structural conditions. Thus, to delineate a complete picture of the metal/bradykinin interaction different structured metal surfaces and specifically mutated analogues should be used.

Table 1. The amino acid sequence of BK and its B_2 receptor antagonists.

Compound	Amino acid sequence									
	0	*1*[a]	*2*[a]	*3*	*4*[a]	*5*	*6*[a]	*7*	*8*	*9*[a]
BK		Arg	Pro	Pro	Gly	Phe	Ser	Pro	Phe	Arg
[D-Arg[0],Hyp[3], Thi[5,8],L-Pip[7]]BK	D-Arg	Arg	Pro	Hyp	Gly	Thi	Ser	L-Pip	Thi	Arg
[D-Arg[0],Hyp[3],Thi[5],D-Phe[7],L-Pip[8]]BK	D-Arg	Arg	Pro	Hyp	Gly	Thi	Ser	D-Phe	L-Pip	Arg

Abbreviations:

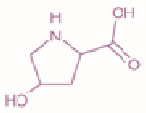

Hyp
L-hydroxyproline

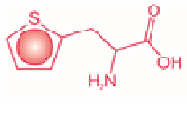

Thi
L-thienylalanine

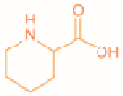

Pip
L-pipecolic acid

[a] *common amino acid in the sequence of all investigated analogues*

Our interest in BK results from the fact that depending on a way of its interaction with the specific B_1 and B_2 receptors, belonging to metabotropic seven-transmembrane G-protein-coupled receptors (GPCRs); therefore, depending on its structure, BK has different biological responses, including respiratory allergic reactions, septic shock, hypertension, hypotensive transfusion reactions, mechanisms of pain, heart diseases, pancreatitis, hereditary and acquired angioedema, Alzheimer disease and carcinoma growth. It also acts as a neuromediator regulator causing natriuresis, which contributes to the drop in blood pressure, and contraction of non-vascular smooth muscle; increasing vascular permeability; raising internal calcium levels in neocortical astrocytes.[31-36]

The determination of the native structure, method of synthesis, and different physiological and pathophysiological properties of BK have contributed to design and synthesis of few generation classes of B_2 BK receptor antagonists.[37-42] The first antagonist for the B_2 BK receptor was [D-Phe[7]]BK.[33] The key structural change in the BK sequence was the replacement of Pro[7] by the D- Phe residue. The [D-Phe[7]]BK analogue was partial agonist with the weak antagonistic activity at the rabbit and guinea pig.[37,38] Another modifications, by both addition of the D-Arg[0] at the BK *N*-terminus blocked enzyme activity and substitution of Pro at position 3 (Pro[3]) of the BK sequence by *L*-hydroxyproline (Hyp[3]) improved the antagonistic properties of these analogues.[37] On the other hand, the replacement of two Phe (Phe[5,8]) by *L*-thienylalanine (Thi[5,8]), unnatural amino acid, gave resistance to enzymatic degradation and reinforced receptor affinity.[39]

Another laboratory has also reported that the substitution at positions 7 and 8 of the [D-Arg[0],Hyp[3],Thi[5,8],D-Phe[7]]BK Stewart's antagonist by L-Pip residue (L-Pip[7]/L-Pip[8]) reduces conformational freedom of the *C*-terminal fragment and changes the character of the relevant part of the molecule from aromatic to aliphatic as well as increases the peptide antagonistic properties in the blood pressure and rat uterus tests.[40] Generally, very potent antagonists have been synthesized when substitutions were incorporated in the BK *C*-terminal ends.[37-42]

Experimental

Peptide synthesis

BK (powder, ≥98% (HPLC)) was purchased from Sigma-Aldrich (Poland).

[D-Arg[0],Hyp[3],Thi[5,8],L-Pip[7]]BK and [D-Arg[0],Hyp[3],Thi[5],D-Phe[7],L-Pip[8]]BK analogues were synthesized by the solid-phase method using the Fmoc-strategy starting from Fmoc-Arg(Pbf)-Wang resin (GL Biochem Shanghai Ltd., 1% DVB, 100– 200 mesh, 0.4 mmol/g).[43] Fmoc was removed by 20% piperidine in DMF. A 3-fold excess of the respective Fmoc-amino acids was activated in situ using TBTU (1 eq)/HOBt (1 eq) in a mixture of DMF/NMP (1:1 v/v) containing 1% Triton, and the coupling reactions were base-catalyzed with NMM (2 eq). The amino acid side-chain-protecting groups were Bu[t] for Hyp and Ser and Pbf for Arg and D-Arg. All of the Fmoc-protected amino acids were commercially available (NovaBiochem, Bad Soden, Germany). Aaa (1-adamantaneacetic acid) was coupled in the final coupling step (for acylated peptides) using the same procedure as that for Fmoc-amino acids. Cleavage of the peptides from the resin with side-chain deprotection was performed by treatment with TFA:H_2O:TIS (95.5:2.5:2.5 v/v/v) for 4 h. The total volume of the TFA filtrate was reduced to approximately 1 mL by evaporation *in vacuum*. The peptides were precipitated with cold diethyl ether and filtered through a Schott funnel. All of the peptides were purified by semi-preparative high-performance liquid chromatography (HPLC).

HPLC was performed on a Waters (analytical and semi-preparative) chromatograph equipped with a UV detector (λ = 226 nm). The purity of the peptides was determined on a Hypersil C_{18} column (5 μm, 100 Å; 250 × 4.6 mm). The solvent systems were [A]

0.1% aqueous trifluoroacetic acid (TFA) and [B] 80% acetonitrile in aqueous 0.1% TFA (v/v). A linear gradient from 20 to 80% of [B] over 30 min was applied for peptides at a flow rate of 1 mL/min. Semi-preparative HPLC was performed using a Waters C_{18} column (15 µm, 100 Å; 7.8 × 300 mm) in a linear gradient from 15 to 45% of [B] for 60 min at a flow rate of 2.5 mL/min. The FAB/MS of the peptides was recorded on a TRIO-3 mass spectrometer at 7 keV with argon as the bombarding gas and on a Bruker BIFLEX III MALDI TOF mass spectrometer (ionization: 337 nm nitrogen laser).

The pharmacological properties of the peptides were examined using two various tests. The antiuterotonic activity was assayed on isolated rat uterus using a modified version of Holton's procedure (rat uterus test; RUT).[44] In the second test, we assessed the antagonistic potency of the analogs by their ability to inhibit the vasodepressor response to exogenous BK in conscious rats (blood pressure test; BPT).[45,46] BK was used as a standard agonist in both tests. For more details, see reference 40.

Ag nanowires synthesis

Ag nanowire solution was synthesized by polyhydric alcohol liquid reducing method in ethylene glycol solution.[47] $AgNO_3$, PVP, $CuCl_2{\cdot}H_2O$, and ethylene glycol were purchased from Sigma Aldrich and were used without further purification. Solutions of 94 mM $AgNO_3$, 4 mM $CuCl_2{\cdot}2H_2O$, and 114 mM PVP were prepared in ethylene glycol. Typically, two batches with 5 ml of ethylene glycol solutions were heated in an oil bath (temperature 150-160 °C) and stirred for 1 hour. Then 40 µl of 4 mM $CuCl_2{\cdot}2H_2O$ was added into the heated ethylene glycol. After 10-15 min. of additional heating 3 ml of a PVP (114 mM) and 3 ml of a $AgNO_3$ (94 mM) solutions in ethylene glycol were added drop-wise at a rate of 27 ml/h using injection pump. The solution was then heated and stirred for another 2 hours. The colour of the solution changed from yellow to gray, which indicated the formation of stable Ag nanowires. The resulting solution was centrifuged in acetone (HPLC grade) in proportion 1:4 at 2000 rpm for 20 min. The supernatant was removed and the solid fraction containing the Ag nanowires was dispersed in 2 ml deionized water and centrifuged at 2000 rpm for 20 min. The centrifugation procedure was repeated two times. The stock solution of the aqueous Ag nanowires has pH = 7.

Ultraviolet–visible spectroscopy measurements

The UV–Vis spectra of an aqueous BK solution, an aqueous Ag nanowires sol, and a peptide/Ag nanowires system (measured after 15 and 120 minutes of mixing) (see Fig. 1) were recorded on a Shimadzu UV-3100 spectrophotometer.

Scanning electron microscope measurements

The SEM images of the Ag nanowires sol were recorded on a SEM instrument, model S-5000 (Hitachi Ltd., Japan), operated at 20 kV (see Fig. 1A and B).

SERS and TERS measurements

Aqueous peptide solutions were prepared by dissolution of peptide in deionized water (18 MΩ·cm). The concentration of the sample was adjusted to 10^{-4} M prior to its being mixed with the colloidal suspended Ag nanowires. 10 microliters of peptide sample was mixed with 20 µl of the Ag nanowires. The mixture was kept for 15 min before the SERS measurement. For TERS measurements after 15 minutes of incubation the mixture was deposited onto a glass plate and dried in a vacuum dryer at 37°C for 30 minutes.

The SERS spectra were collected with Renishaw spectrometer (model inVia) operating in confocal mode combined with a Peltier cooled CCD detector and a Leica microscope (50x long-distance objective). The 514.5 nm line of Ar-ion laser (Renishaw) was used as an excitation sources. The lasers power at the laser output was set at about 15 mW. The typical exposure time for each SERS measurement was 40 s with four accumulations (series of 4 spectra, each accumulated 40 s = 160 s).

The SERS spectra were measured at ten spots on the surface of the colloidal suspended Ag nanowires. The series of spectra were nearly identical (highly reproducible), except for small differences (up to 5%) in some band intensities.

The TERS spectra were measured by an instrument consisting of a reflection-mode Raman microscope (Photon Design Inc.) equipped with a CCD detector (Princeton Instrument) and an AFM instrument (Photon Design, Nanostar NFRSM800). This system was arranged to introduce excitation light from the top of the sample and to collect backscattered signals using a 90x objective lens (numerical aperture, NA = 0.71). The 514.5 nm line from an Ar-ion laser (Spectra Physics, Stabilite 2017-06S) was used as the excitation source. The laser power at the sample point was 0.1 mW. Polarization of the laser was parallel to the tip. A TERS needle coated with Ag (UNISOKU Co. Ltd.) was attached to the quartz tuning fork of a shear-force-based AFM at an angle of 45°. The tip radius of the probe was about 100 nm (spatial resolution of experiments about 100 nm). The TERS tip-approached the sample using the non-contact mode. A Raman signal was first collected under the tip-retracted conditions (distance of 230 nm), and then, under the tip-approached conditions (distance of 1–2 nm) at the same point. The typical exposure time for each the SERS measurement was 20 s with eight accumulations (series of 10 spectra each of 20 s = 200 s) under the tip-retracted and tip-approached conditions.

Spectral analysis

The spectral analysis was performed using the GRAMS/AI 8.0 program (Thermo Scientific).

Second derivatives of the TERS spectra were calculated in the range of the amide I and II bands using the Savitzky-Golay algorithm[48] that produces the least squares best fit of the data to the selected polynomial. The number of convolution points can range from 5 to 10,000, although values greater than the number of points across a peak are not normally used. Only odd numbers are used for number of convolution points and even values are rounded up. The number of convolution points and degree adopted in this work was set at 10 and 5, respectively. These parameters did not distort the spectra. However, a larger number of convolution points provided to the more smoothing result.

Results and discussion

Optical properties of the Ag nanowires

Fig. 1 presents the excitation (UV-Vis) spectrum and SEM images at different magnification (A: scale 8.56 µm and B: scale 667 nm) of an aqueous Ag nanowires solution. As is evident form this figure,

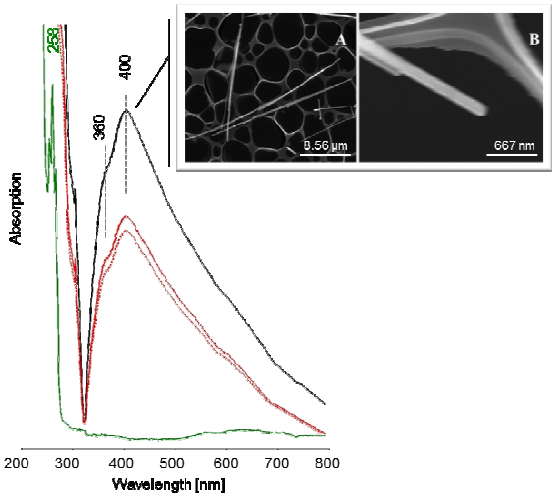

Figure 1. The excitation (UV-Vis) spectra of BK in the aqueous solution (green line) and the aqueous Ag nanowires (black line) and peptide/Ag nanowires system (red solid and dashed line; measured after 15 and 120 minutes of mixing, respectively) in the 200 – 800 nm range and SEM images of the Ag nanowires solutions (A (20.0 kV x3.51 k, scale 8.56 µm) and B (20.0 kV x45.0 k, scale 667 nm)).

individual rather cylindrical nanowires (2 – 50 µm of length and 350 – 500 nm of diameter), showing the very broad plasmon resonance band in the wavelength range of 350 – 500 nm, are randomly oriented. The observed 360 and 400 nm maxims could be assigned to bulk Ag film and transverse plasmons of the Ag nanowire arrays, respectively.[49] The significant broadening of the 400 nm band is probably due to the coupling of the electromagnetic waves emitted by the neighbouring Ag nanowires.[50] The addition of peptide (10 µL of 10^{-4} M) to the Ag nanowires solution (20 µL) produced decrease in the absorbance of 350 – 500 nm band and did not trigger nanowires aggregation.

TERS onto the Ag nanowires

Fig. 2 presents the AFM images of the contact surfaces of the colloidal suspended Ag nanowires (scale bar 500 nm) with the marked probing points where the TERS spectra were measured and the surface characteristic diagrams: A for BK (points from A1 to A4), B for [D-Arg^0,Hyp^3,Thi^{5,8},L-Pip^7]BK (points from B1 to B4), and C for [D-Arg^0,Hyp^3,Thi^5,D-Phe^7,L-Pip^8]BK (points from C1 to C4). As is evident from this figure, drying of the aqueous Ag nanowires solutions did not produce the aggregation of the Ag nanowires. For these probing points, Figs. 3 – 5 show the selected TERS spectra of BK and its two mutated [D-Arg^0,Hyp^3,Thi^{5,8},L-Pip^7]BK and [D-Arg^0,Hyp^3,Thi^5,D-Phe^7,L-Pip^8]BK analogues measured under the tip-approached conditions. Figs. 3 – 5 also show the SERS spectra (red dashed line) collected at the probing points no. 1 (A, B, and C) and in the Ag nanowires aqueous solution (insets (4)). The comparison of the peptides respective SERS and TERS spectra at the probing point no. 1 evidences the similar set of bands. Therefore, due to the weaker strength of the SERS signals in respect to the significantly enhanced TERS signals, analysis is based on the TERS spectra. To enhance resolution of the TERS spectra measured at the probing points no. 1 (complex spectra containing overlapped bands) the second-derivative (in the range 1700 – 950 cm^{-1}) spectra were calculated (Figs. 3 – 5, Insets (1)). Also, TERS spectra were calculated (Fig. 3 – 5, Insets (2)) by subtracting the respective spectrum collected under the tip-retracted conditions from that measured under the tip-approached conditions.

The spectral positions of the enhanced bands in the TERS spectra, given in wavenumbers, together with the proposed vibrational assignments are summarized in Table 2. This assignment leans on our earlier detailed SERS and TERS studies on BK and its Phe-D_5 isotopically labeled and specifically mutated analogues deposited onto the roughened in the oxidation-reduction cycles (ORC) Ag, Au, and Cu electrodes (at different applied electrode potential)[51,52] and onto the Ag or Au colloidal nanoparticles surfaces.[30,53] Further information about bands allocation was obtained also from the published normal mode analysis of free or metal-bound BK analogs,[30,51-54] piperidine (Pip),[55-57] and thiophene (Thi).[58,59]

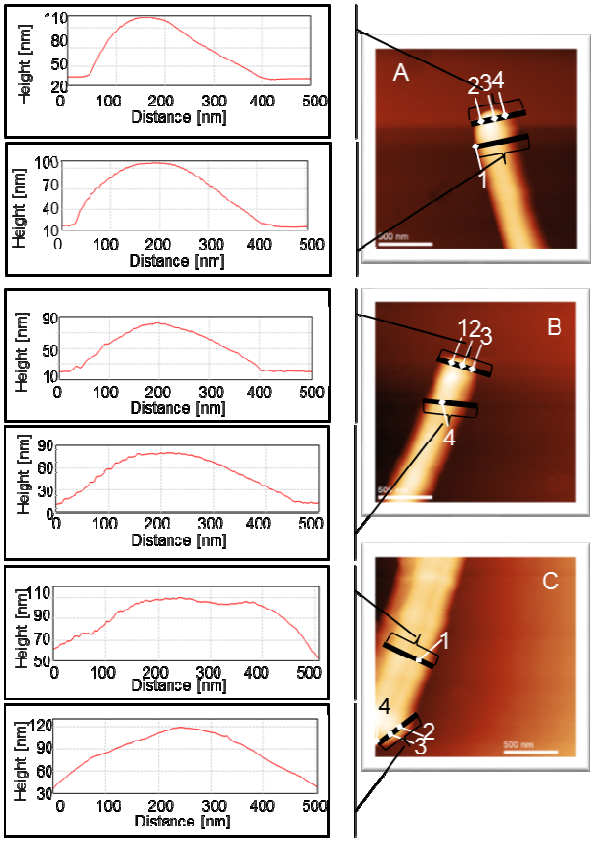

Figure 2. The AFM images of the peptide-Ag nanowires systems with probing spots where the TERS spectra were collected and the surface characteristic diagrams: BK (A), [D-Arg^0,Hyp^3,Thi^{5,8},L-Pip^7]BK (B), and [D-Arg^0,Hyp^3,Thi^5,D-Phe^7,L-Pip^8]BK (C). Measurement conditions: magnification 500 nm.

It has to be noted that the 1625, 1602/1574, 1442, 1390, 1308, 1282, 1242, 1215, 1033, and 1003 cm^{-1} bands (Table 2) mainly due to the amide I/$\delta_{as}(NH_2)$, $\nu_{8b/8a}$, ν_{19b}, $\nu_s(COO^-)$, ν_{14}, ν_3, amide III, ν_{7a}, ν_{18a}, and ν_{12} modes, respectively, are enhanced in the TERS spectra

of BK; however, they show only slightly different intensities (for this reason, the representative TERS spectrum is presented and discussed (Fig. 3, inset (2)). The aforementioned spectral features suggest that the carboxylate group of Arg[9], the Phe ring(s) (Phe[5,8]), and amide bond, being arranged in a similar manner in respect to the colloidal suspended Ag nanowire surface at each probing point, are involved in the interaction with this surface. These observations are in good agreement with the structure model of BK bound to the human B_2 receptor determined by the solid-state NMR spectroscopy[60] and our previous results obtained onto the colloidal suspended Ag nanoparticles surface[30] that depict the same peptide fragment, which interacts with both the receptor and metal surface. Based on the analysis of the changes in the wavenumber, intensity, and full width at half band maximum (fwhm) of the aforementioned bands among the respective Raman and TERS spectra, the following conclusions can be drawn about the arrangement of the individual fragments on the colloidal suspended Ag nanowire surface.

The low intensity of the 1003 cm^{-1} TERS signal (Fig. 3) in comparison to that in the corresponding Raman spectrum[51,54] implies that the Phe ring(s) either adopted more or less tilted orientation with respect to the cylindrical Ag nanowire surface or is(are) moved away from this surface. Although no shift in wavenumber and small broadening (by 6 cm^{-1}) of this band in comparison to those in the Raman spectrum allow to state that Phe is tilted in some proximity to the Ag nanowire surface. This proposed orientation of Phe corresponds to its behaviour in an aqueous colloidal Au and Ag sols[30,53] and onto the colloidal suspended Ag nanoparticles surface.[30] However, based on the comparison of the enhancement, broadness, and shift in frequency of the ν_{12} band between the BK TERS spectra onto the nanospherical and nanowire surface it seems that the tilt angle between the Phe ring plane and the Ag surface normal is bigger for suspended Ag nanoparticles surface than the Ag nanowire surface.

The strong enhancement of the 1390 cm^{-1} band (fwhm = 36 cm^{-1}) (Fig. 3, inset (2)), that is weakly scattered at 1405 cm^{-1} (fwhm = 14 cm^{-1}) in the BK Raman spectrum, allows to conclude that the *C*-terminal deprotonated carbonyl moiety of BK remained in the close proximity to the colloidal suspended Ag nanowire surface in a manner, which promotes the interaction of the lone pair of electrons on oxygen(-s) with this surface. The appearance of 1512 and 233 cm^{-1} spectral features due to the antisymmetric stretching vibrations of the $-COO^-$ group and symmetric O–Ag vibrations, respectively, in the BK TERS spectrum support the $-COO^-\cdots$Ag interactions. In addition, the frequencies of the $\nu_{as}(COO^-)$ and $\nu_s(COO^-)$ vibrations differ by 122 cm^{-1}, what indicates that the BK carboxylate moiety binds to the Ag nanowire surface through the only one oxygen atoms of the carboxylate group,[61,62] similar as in the case of this peptide deposited onto the colloidal suspended Ag nanoparticles surface[30]. Although based on the enhancement of

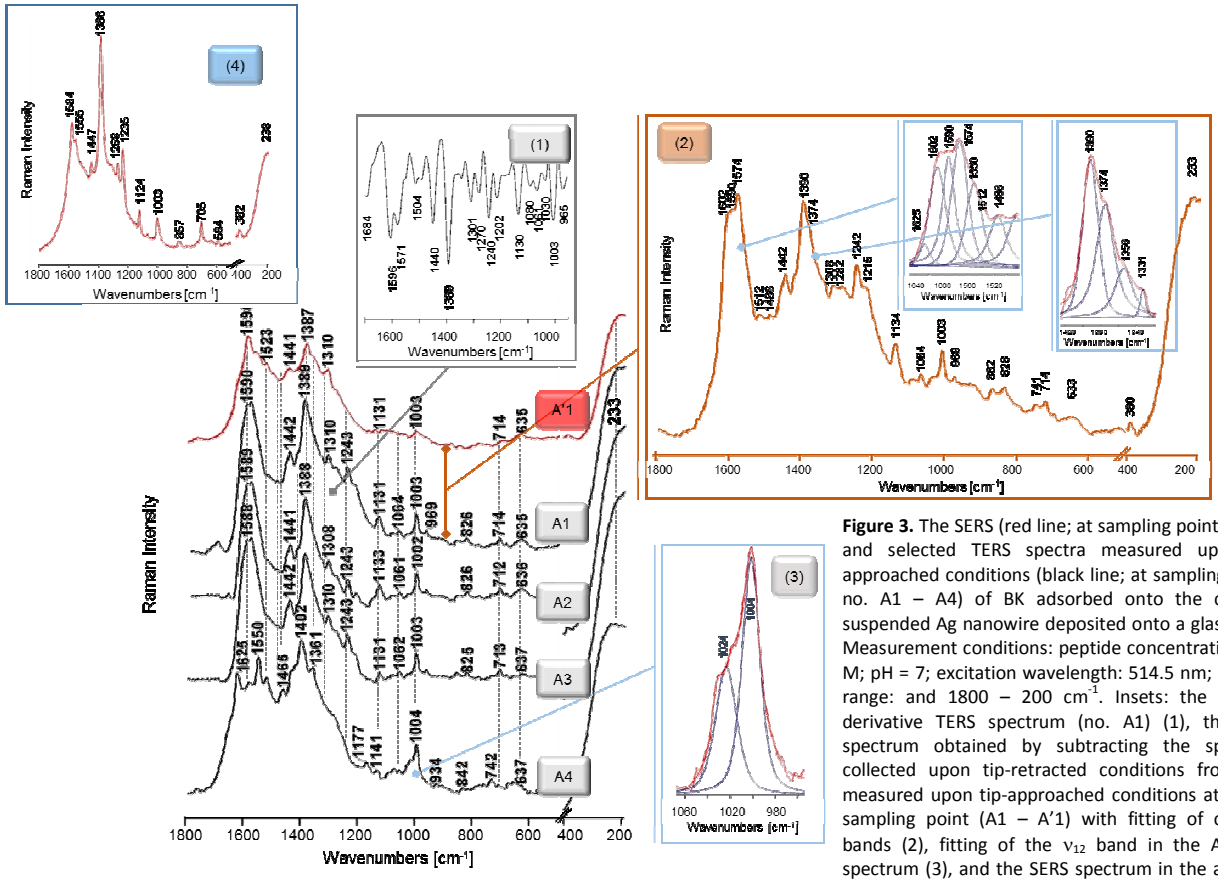

Figure 3. The SERS (red line; at sampling point no. A1) and selected TERS spectra measured upon tip-approached conditions (black line; at sampling points no. A1 – A4) of BK adsorbed onto the colloidal suspended Ag nanowire deposited onto a glass plate. Measurement conditions: peptide concentration: 10^{-5} M; pH = 7; excitation wavelength: 514.5 nm; spectral range: and 1800 – 200 cm^{-1}. Insets: the second-derivative TERS spectrum (no. A1) (1), the TERS spectrum obtained by subtracting the spectrum collected upon tip-retracted conditions from that measured upon tip-approached conditions at the A1 sampling point (A1 – A'1) with fitting of complex bands (2), fitting of the ν_{12} band in the A4 TERS spectrum (3), and the SERS spectrum in the aqueous solution (4).

Table 2. Wavenumbers and proposed band assignments for the TERS spectra of BK and its B_2 receptor antagonists: [D-Arg^0,Hyp^3,Thi^{5,8},L-Pip^7]BK and [D-Arg^0,Hyp^3,Thi^5,D-Phe^7,L-Pip^8]BK adsorbed onto the colloidal suspended Ag nanowires.

Proposed assignment	Wavenumber [cm^{-1}] in TERS		
	A1-A'1	B1-B'1	C1-C'1
Amide I and/or Arg [$\delta_{as}(NH_2)$]	**1625**^{d}	1625^d	1625^d
Phe/Thi [ν_{8a}]	**1602**	1602^s	1600
Arg [ν_{as}(C=N)]	**1590**	1586	–
Phe/Thi [ν_{8b}]	**1574**	1572^s	1576
Arg [δ(NH)] and/or Amide II	**1550**^{d}	–	–
Thi [ν_{8b}]	–	1542^s	1548
Arg [$\nu_{as}(COO^-)$]	**1512**	1513	1528
Phe [ν_{19a}] or Thi [ν(CC)]	**1486**	1476	–
Phe/Thi [ν_{19b}] and Pip [$\rho_s(CH_2)$]	**1442**	1460	1453
Thi [(ν(CH=C) + ν(CS) + ρ_r(CH)]	–	1401^d	–
Arg [$\nu_s(COO^-)$]	**1390**	1386^d	-
Pip combination	–	–	1399
Arg [$\rho_w(CH_2)$ and ν(C–N)]	**1374**^{s}	1373^d	1378^d
	–	–	1360
Arg [$\rho_w(CH_2)$]	**1331**^{s}	1340	1341
Phe [ν_{14}] or Pip [$\rho_w(CH_2)$]	**1308**	1316	1302
Phe [ν_3] or Pip [$\rho_t(CH_2)$]	**1282**	1283	1286
Amide III or Pip [$\rho_t(CH_2)$]	**1242**	1254	1250
Phe [ν_{7a}] or Pip	**1215**	1210	–
Thi [ν(C=S)]	–	1196	–
Arg [δ(NH)] and/or ν_{as}(CNC)	**1134**	1135	1143
Arg [ν_s(C–C) + ν(C–N)]	**1087**	1086	–
Arg [ν(C–N)]	**1064**	1065	1076
Phe [ν_{18a}]	**1033**	–	–
Thi [ν(C–C) + ρ_r(CH)]	–	1036	–
Pip [skeletal stretch]	–	–	1010
Phe [ν_{12}]	**1003**	–	995
Thi [ρ_r(CH)]	–	996	–
ν_{as}(CCC) + **Phe [ρ_{oopw}(CH)]**	**969**	–	–
Arg [$\rho_r(CH_2)$]	**862**	–	–
Arg[δ(NH)]	**828**	–	–
Thi [ρ_w(CH)]	–	808	–
Arg [δ(NH)]	**741**	737	–
Arg [$\rho_r(CH_2)$]	**714**	–	–
Amide	**633**	657	654
Thi [ν(C–S)+δ(ring)]	–	571	590
ν(Ag–N)	380	379	378
ν(Ag–O) and ν(Ag–N)	233	228	227

Abbreviations: ν – stretching, ν_s and ν_{as} – symmetric and asymmetric stretching, respectively, δ - deformation, ρ_w – wagging, ρ_t – twisting, ρ_s –scissoring, and ρ_r – rocking vibrations; Arg – L-arginine, Phe – L-phenylalanine, Thi – L-thienylalanine, and Pip – L-pipecolic acid; ^{s} – shoulder and ^{d} – fitting

the $\nu_s(COO^-)$ and ν(O-Ag) bands it seems that the –COO^- group binds stronger to the colloidal suspended Ag nanoparticles surface than to the Ag nanowires surface .

Additionally, in the BK TERS spectrum onto the colloidal suspended Ag nanowire surface (Fig. 3, inset (2)), similarly to the TERS spectrum on the colloidal suspended Ag nanoparticles surface,[30] bands due to the Arg residue(s) vibrations (at 1374, 1342, 1134, 1087, 862, 828, 741, and 714 cm^{-1} (see Table 2 for the proposed Ag nanowire surface (Fig. 3, inset (2)), are enhanced. These spectral features are mainly due to the N–H, C–N, and –CH_2– guanidine moieties oscillations. Thus, it seems that the H_2N–C–NH–CH_2– fragment of Arg is adsorbed onto the colloidal suspended Ag nanowire surface. The around 380 cm^{-1} (ν(Ag–N)) band supports this statement.

In the case of the [D-Arg^0,Hyp^3,Thi^{5,8},L-Pip^7]BK analogue, almost all of the spectral features in its TERS spectrum (Fig. 4, inset (2)) could be correlated, without difficulty, to the Thi and Arg residues vibrations. These include the TERS signals at 1602, 1572, 1542, 1482, 1460, 1401, 1196, 996, 808, and 571 cm^{-1} due to Thi and at 1586, 1513, 1386, 1373, 1340, 1135, 1065, and 737 cm^{-1} due to Arg (see Table 2 for the band assignment). The 1602, 1586, and 1572 cm^{-1} and the 1401, 1386, and 1373 cm^{-1} bands overlapped giving two intense bands. These two bands together with the 996 cm^{-1} spectral feature dominate the [D-Arg^0,Hyp^3,Thi^{5,8},L-Pip^7]BK TERS spectrum and; thus, imply that both these residues are mainly involved (Thi through the aromatic ring and Arg via the imine and carbonyl groups) in the interaction of [D-Arg^0,Hyp^3,Thi^{5,8},L-Pip^7]BK with the colloidal suspended Ag nanowire surface. The frequency of the carbonyl group symmetric stretching vibration (at 1386 cm^{-1}) and the difference in the frequencies between ν_{as}(COO) and ν_s(COO) (142 cm^{-1}) suggest that the deprotonated carbonyl group serves rather as a bidentate coordination ligand. Because Arg^9 at the *C*-terminal end of the analogue is the only one residue that contains the carbonyl moiety and both Arg and Thi^8 bind to Ag it seems that only Arg at position 9 in the amino acid sequence, rather than all three Arg residues (D-Arg^0, Arg^1, and Arg^9), interacts with the colloidal suspended Ag nanowire surface. This statement could be supported be the weak enhancement of the amide bond (at 1638, 1254, and 657 cm^{-1}) vibrations. In addition, knowing that the 1401 (ν(CH=C) + ν(CS) + ρ_r(CH)), 1196 (ν(C=S)), and 571 cm^{-1} (ν(CS) + δ(ring)) TERS signals are (1) influenced by the vibrations of this part of the Thi ring, which has the sulfur atom, (2) strengthened in comparison to those in the [D-Arg^0,Hyp^3,Thi^{5,8},L-Pip^7]BK Raman spectrum, and (3) broadened (by 11 – 20 cm^{-1}) the following conclusion could be made. The Thi ring, being tilted or perpendicular to the colloidal suspended Ag nanowire surface, is directed to this surface through the sulfur atom.

The TERS spectrum of [D-Arg^0,Hyp^3,Thi^5,D-Phe^7,L-Pip^8]BK (Fig. 5, inset (2)) is dominated by the Arg side-chain (1528, 1378, 1341, 1302, 1286, 1143, and 1076 cm^{-1}) and the D-Phe^7 (1600, 1576, and 995 cm^{-1}) and Pip^8 (1399 and 1010 cm^{-1}) rings vibrations (see Table 2 for detailed band allocation). Thus, onto the colloidal suspended Ag nanowire surface the [D-Arg^0,Hyp^3,Thi^5,D-Phe^7,L-Pip^8]BK analog behaves differently than BK and [D-Arg^0,Hyp^3,Thi^{5,8},L-Pip^7]BK, which interacts with this surface through the last two amino acids in the peptide sequence. For [D-Arg^0,Hyp^3,Thi^5,D-Phe^7,L-Pip^8]BK, the D-Phe residue at the third position from the peptide *C*-end assists in the peptide interaction with the colloidal suspended Ag nanowire surface. This is not surprising, since it is known that aromatic rings have high affinity to the metal surface.

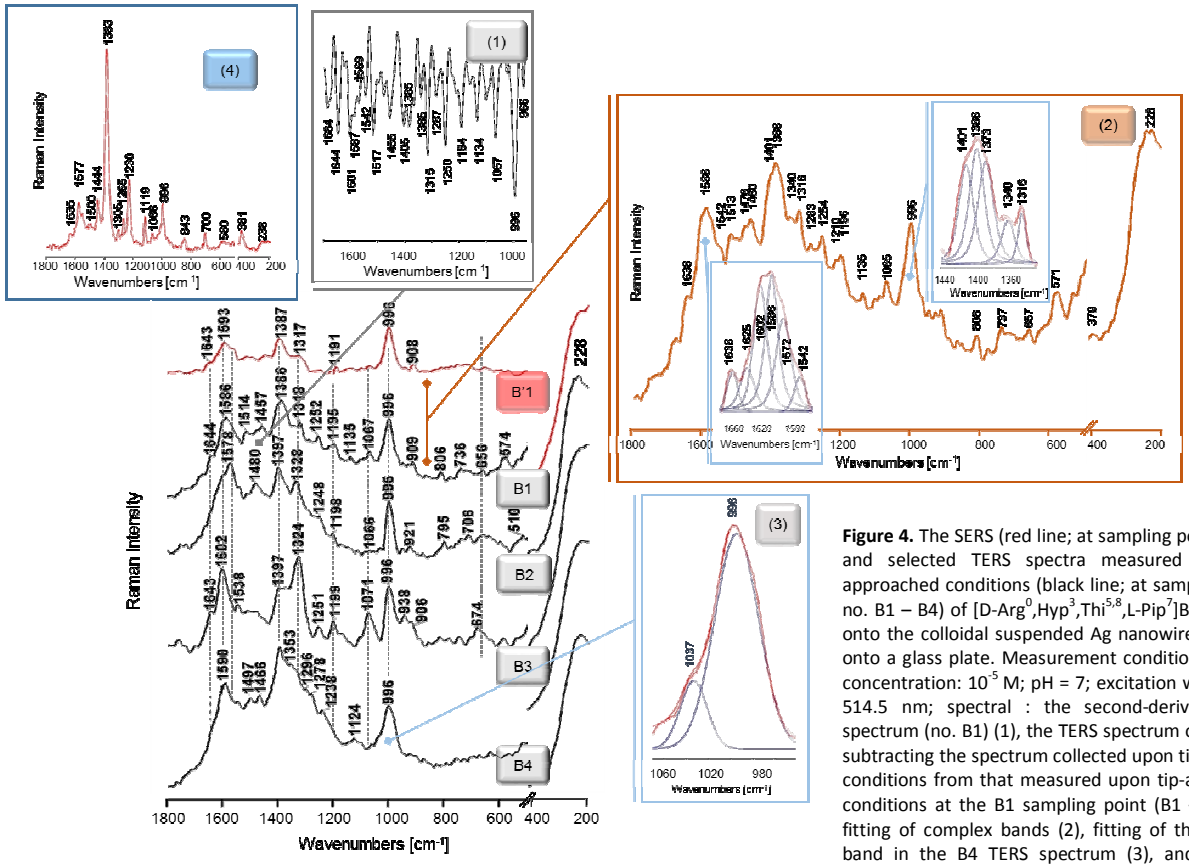

Figure 4. The SERS (red line; at sampling point no. B1) and selected TERS spectra measured upon tip-approached conditions (black line; at sampling points no. B1 – B4) of [D-Arg^{0},Hyp^{3},Thi^{5,8},L-Pip^{7}]BK adsorbed onto the colloidal suspended Ag nanowire deposited onto a glass plate. Measurement conditions: peptide concentration: 10^{-5} M; pH = 7; excitation wavelength: 514.5 nm; spectral : the second-derivative TERS spectrum (no. B1) (1), the TERS spectrum obtained by subtracting the spectrum collected upon tip-retracted conditions from that measured upon tip-approached conditions at the B1 sampling point (B1 – B'1) with fitting of complex bands (2), fitting of the 996 cm^{-1} band in the B4 TERS spectrum (3), and the SERS spectrum in the aqueous solution (4).

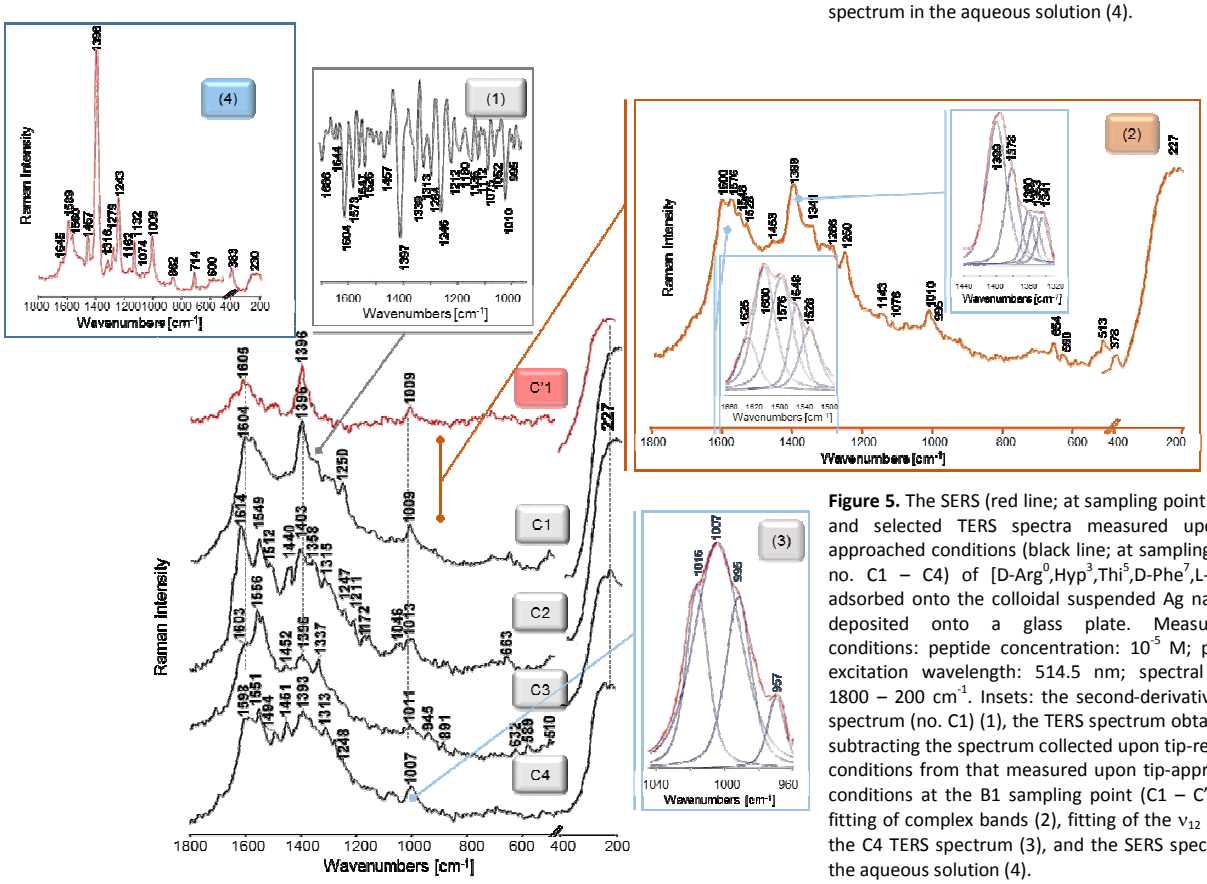

Figure 5. The SERS (red line; at sampling point no. C1) and selected TERS spectra measured upon tip-approached conditions (black line; at sampling points no. C1 – C4) of [D-Arg^{0},Hyp^{3},Thi^{5},D-Phe^{7},L-Pip^{8}]BK adsorbed onto the colloidal suspended Ag nanowire deposited onto a glass plate. Measurement conditions: peptide concentration: 10^{-5} M; pH = 7; excitation wavelength: 514.5 nm; spectral range: 1800 – 200 cm^{-1}. Insets: the second-derivative TERS spectrum (no. C1) (1), the TERS spectrum obtained by subtracting the spectrum collected upon tip-retracted conditions from that measured upon tip-approached conditions at the B1 sampling point (C1 – C'1) with fitting of complex bands (2), fitting of the ν_{12} band in the C4 TERS spectrum (3), and the SERS spectrum in the aqueous solution (4).

The low intensity, shift in wavenumber (by 7 cm^{-1}), and broadening (by 11 cm^{-1}) of the 995 cm^{-1} TERS band in comparison to the Raman values point out on the more or less flat orientation of the D-Phe^7 ring in respect to the colloidal suspended Ag nanowire surface. On the other hand, the lack of the $\nu_{as}(COO^-)$ and $\nu_s(COO^-)$ bands suggests that the carbonyl group of Arg^9 does not coordinate to Ag. This is probably due to the arrangement of the whole molecule at the Ag surface forced by D-Phe^7 ···Ag interaction.

It is worth mentioning that in generally, the SERS spectra in the aqueous Ag nanowires solution (insets (4)) are simpler than the corresponding TERS spectra onto the colloidal suspended Ag nanowires deposited onto a glass plate (insets (2)). All the main bands in the BK SERS spectrum (Fig. 3, inset (4)), similar as in the TERS spectrum, are due to the vibrations of Arg (1555 cm^{-1} – δ(NH) and/or Amide II; 1386 cm^{-1} – $\nu_s(COO^-)$; 1235 cm^{-1} – Amide III; 1124 cm^{-1} – δ(NH); 857 and 705 cm^{-1} – $\rho_r(CH_2)$) and Phe (1584 cm^{-1} – ν_{8a}; 1447 cm^{-1} – ν_{19b}; 1268 cm^{-1} – ν_3; 1003 cm^{-1} – ν_{12}), what support the general adsorption mode of BK through the *C*-terminal –Phe–Arg fragment. Although the intensity of the corresponding Arg bands mainly differs between the SERS and TERS spectra, pointing out the main changes in the orientation/strength of interactions between carboxylate and guanidine groups and both the Ag surfaces. The similar changes between the SERS and TERS spectra are observed for [D-Arg^0,Hyp^3,$Thi^{5,8}$,L-Pip^7]BK (Fig. 4, insets (4) and (2)). However, for [D-Arg^0,Hyp^3,Thi^5,D-Phe^7,L-Pip^8]BK it seems the spectral profile experiencing the biggest alternation upon the change of the environment. This change is primarily due to the adsorption of this peptide through the carboxylic group onto the colloidal suspended Ag nanowires deposited onto a glass plate (Fig. 5, inset (2)) and via the pipecolic ring in the aqueous Ag nanowires solution (Fig. 5, inset (4)).

A noteworthy fact is that the strong and broad 1210 – 1450 and 1450 – 1580 cm^{-1} TERS bands due to the 'D peak' and 'G peak', respectively, of the hydrogenated amorphous carbon contamination, which is formed on a metal surface during rapid photodecomposition (by the highly enhanced electromagnetic field) of the adsorbed organic compound influence the TERS spectra.[63-65]

Conclusions

The adsorption mode of BK and its two potent B_2 BK receptor antagonists [D-Arg^0,Hyp^3,$Thi^{5,8}$,L-Pip^7]BK] and [D-Arg^0,Hyp^3,Thi^5,D-Phe^7,L-Pip^8]BK onto the colloidal suspended Ag nanowires ((2 – 50 μm of length and 350 – 500 nm of diameter) was defined by TERS. Based on the analysis of the changes in the wavenumber, intensity, and full width at half band maximum of the proper bands among the respective Raman and TERS spectra the possible manner of binding to the colloidal suspended Ag nanowire surface of the investigated peptides was presented in Fig. 6. Also, the following conclusions were drawn:

i) Two last amino acids in the *C*-terminal end of BK and [D-Arg^0,Hyp^3,$Thi^{5,8}$,L-Pip^7]BK] are involved in the interaction between peptide and Ag surface; whereas the D-Phe^7, Pip^8, and Arg^9 residues of [D-Arg^0,Hyp^3,Thi^5,D-Phe^7,L-Pip^8]BK interact with Ag. Therefore, the TERS experiments highlight the importance of the peptides *C*-terminal part in the adsorption process onto the colloidal suspended Ag nanowire surface. Also, they prove that the same peptide fragments interact with both the colloidal suspended Ag nanowire surface and BK receptors.[60]

ii) The carboxylate (through one of the oxygens) and guanidine groups (via the H_2N–C–NH–CH_2– fragment) of Arg^9, the Phe ring(s) (Phe $^{5/8}$, in tilted orientation of the rings), and amide bond between Phe and Arg of BK are mainly involved in the BK interaction with the colloidal suspended Ag nanowires, what is in good agreement with the previous data.[30,60] However, the Phe orientation on Ag and strength of $-COO^-$ ···Ag interactions depend upon the type of the colloidal suspended Ag substrate. Onto the Ag nanoparticles surface Phe is more tilted in respect the surface normal than onto the Ag nanowires surface. The interaction of the carboxylate group with Ag is stronger for the nanowires surface than for the nanoparticles surface. Thus, we provided one more evidence that nanostructure of a metallic surface and hence controlled distribution of the metal surface plasmon influence the surface geometry of the residues interacting with the metal surface.

iii) The Thi^8 and Arg^9 residues adsorb on the colloidal suspended Ag nanowires for [D-Arg^0,Hyp^3,$Thi^{5,8}$,L-Pip^7]BK]. The Thi^8 ring, being perpendicular to the colloidal suspended Ag nanowire surface, binds preferentially by a lone electron pair on the sulfur atom, whereas the $-COO^-$ group binds through its both oxygen atoms to the Ag nanowires.

iv) The substitution of Pip^7 by D-Phe^7 and Thi^8 by Pip^8 in the [D-Arg^0,Hyp^3,Thi^5,D-Phe^7,L-Pip^8]BK analogue) leads to the significant changes in the adsorption process onto the colloidal suspended Ag nanowire surface of this analogue. Arg^9 and L-Pip^8 as well as D-Phe^7 participate in the adsorption process. The D-Phe^7 ring adopts the more or less flat orientation onto the Ag nanowire surface. This interaction probably pulled the $-COO^-$ group away from the Ag nanowire surface.

i) The TERS studies of BK and its two potent B_2 BK receptor antagonists showed that the bands of the same peptide fragments having the same orientations with respect the colloidal suspended Ag nanowire surface arise from the different probing points onto the Ag surface. Thus, the manner of the peptide adsorption depends only from the peptide modifications and not from the place of binding (the same adsorption geometry).

ii) The TERS experiments demonstrated clearly the feasibility of the TERS technique for studying complex biological molecules.

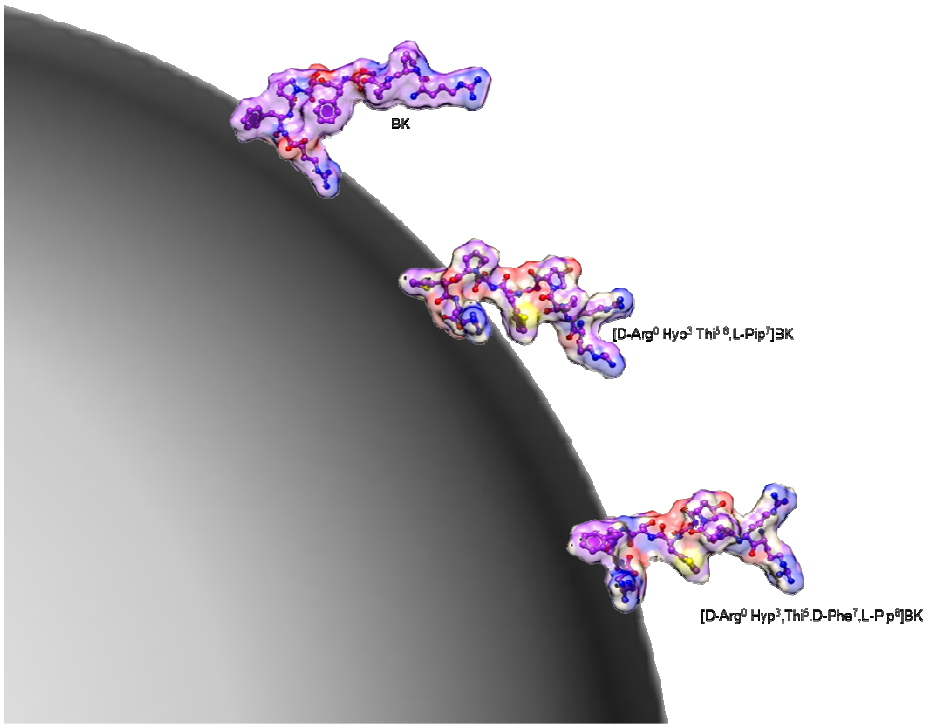

Figure 6. Possible manner of binding onto the colloidal suspended Ag nanowire surface of the investigated peptides.

Conflict of Interests

The authors have no conflict of interests to declare.

Acknowledgments

This work was supported by the National Research Center of the Polish Ministry of Science and Higher Education (Grant No. N N204 354840 to Edyta Proniewicz and Grant No. 2012/05/N/ST4/00175 to Dominika Święch). SM acknowledges support from the European Regional Development Fund within the Regional Operational Programme for Kujawsko-Pomorskie Voivodeship for the years 2007-2013 and the national budget of Poland (project #RPKP 05.04.00-04-006/13).

Notes and references

1 R. M. Stöckle, Y. D. Suh, V. Deckert and R. Zenobi, *Chem. Phys. Lett.*, 2000, **318**, 131.
2 M. S. Anderson, *Appl. Phys. Lett.*, 2000, **76**, 3130.
3 N. Hayazawa, Y. Inouye, Z. Sekkat and S. Kawata, *Optic. Comm.*, 2000, **183**, 333.
4 B.-S. Yeo, J. Stadler, T. Schmid, R. Zenobi and W. Zhang, *Chem. Phys. Lett.*, 2009, **472**, 1.
5 K. F. Domke and B. Pettinger, *Chem. Phys. Chem.*, 2010, **11**, 1365.
6 M. Paulite, C. Blum, T. Schmid, L. Opilik, K. Eyer, G. C. Walker and R. Zenobi, *ACS Nano*, 2013, **7**, 911.
7 D. Kurouski, T. Deckert-Gaudig and V. Deckert, *J. Am. Chem. Soc.*, 2012, **134**, 13323.
8 M. Asghari-Khiavi, B. R. Wood, P. Hojati-Talemi, A. Downes, D. McNaughton and A. Mechler, *J. Raman Spectrosc.*, 2012, **43**, 173 .
9 B. A. Snopok, *Theor. Exp. Chem.*, 2012, **48**, 283.
10 K. A. Willets and R. P. Van Duyne, *Annu. Rev. Phys. Chem.*, 2007, **58**, 267.
11 K. Kneipp, *Phys. Today*, 2007, **60**, 40.
12 K. F. Domke, D. Zhang and B. Pettinger, *J. Am. Chem. Soc.*, 2006, **128**, 14721.
13 W. Zhang, B.-S. Yeo, T. Schmid and R. Zenobi, *J. Phys. Chem. C*, 2007, **111**, 1733.
14 M. D. Sonntag, J. M. Klingsporn, L. K. Garibay, J. M. Roberts, J. A. Dieringer, T. Seideman, K. A. Scheidt, L. Jensen, G. C. Schatz and R. P. Van Duyne, *J. Phys. Chem. C*, 2012, **116**, 478.
15 L. Opilik, T. Bauer, T. Schmid, J. Stadler and R. Zenobi, *Phys. Chem. Chem. Phys.*, 2011, **13**, 9978.
16 M. Paulite, C. Blum, T. Schmid, L. Opilik, K. Eyer, G. C. Walker and R. Zenobi, *ACS Nano*, 2013, **7**, 911.
17 J. Steidtner and B. Pettinger, *Phys. Rev. Lett.*, 2008, **100**, 236101.
18 T. Schmid, B.-S. Yeo, G. Leong, J. Stadler, and R Zenobi, *J. Raman Spectrosc.*, 2009, **40**, 1392.
19 T. Suzuki, X. Yan, Y. Kitahama, H. Sato, T. Itoh, T. Miura and Y. Ozaki, *J. Phys. Chem. C*, 2013, **117**, 1436.
20 S. Vantasin, I. Tanabe, Y. Tanaka, T. Itoh, T. Suzuki, Y. Kutsuma, K. Ashida, T. Kaneko and Y. Ozaki, *J. Phys. Chem. C*, 2014, **118**, 25809.
21 K. D. Alexander and Z. D. Schultz, *Anal. Chem.*, 2012, **84**, 7408.
22 A. Rasmussen and V. Deckert, *J. Raman Spectrosc.*, 2006, **37**, 311.

23 E. Bailo and V. Deckert, *Ange. Chem. Int. Ed.,* 2008, 1658.
24 P. Hermann, A. Hermelink, V. Lausch, G. Holland, L. Möller, N. Bannert and D. Naumann, *Analyst***,** 2011,**136**, 1148-1152.
25 T. Schmid, A. Messmer, B.-S. Yeo, W. Zhang and R. Zenobi, *Anal. Bioanal.Chem.* 2008**, 391**, 1907.
26 R. Bohme, M. Richter, D. Cialla, P. Rosch, V. Deckert and J. Popp, *J. Raman Spectrosc.,* 2009, **40**, 1452.
27 M. Paulite, C. Blum, T. Schmid, L. Opilik, K. Eyer, G. C. Walker and R. Zenobi, *ACS Nano*, 2013, 7, 911.
28 T. Deckert-Gaudig and V. Deckert, *J. Raman Spectrosc.* 2009, **40**, 1446.
29 C. Blum, T. Schmid, L. Opilik, S. Weidmann, S. R. Fagerer and R. Zenobi, *J. Raman Spectrosc*. 2012, **43**, 1895.
30 D. Święch, Y. Ozaki, Y. Kim and E. Proniewicz, *Phys. Chem. Phys. Chem.*, 2015, **17**, 17140.
31 W. Xiong, J. Chao and L. Chao, *Hypertension,* 1995, **25**, 715.
32 M. E. Moreau, N. Garbacki, G. Molinaro, N. J. Brown, F. Marceau and A. Adam, *J. Pharmacol. Sci.,* 2005, **99**, 6
33 L. M. F. Leeb-Lundberg, F. Marceau, W. Müller-Esterl, D. J. Pettibone and B. L. Zuraw, *Mol. Pharmacol*., 2007, **71**, 494.
34 M. Maurer, M. Bader, M. Bas, F. Bossi, M. Cicardi, M. Cugno, P. Howarth, A. Kaplan, G. Kojda, F. Leeb-Lundberg, J. Lötvall and M. Magerl, *Allergy,* 2011, **66**, 1397.
35 J. M. Stewart, *Curr. Pharm. Design,* 2003, **9,** 2036.
36 J. S. Taub, R. Guo, L. M. Leeb-Lundberg, J. F. Madden and Y. Daaka, *Cancer Res*., 2003, **63**, 2037.
37 R. J. Vavrek and J. M. Stewart, *Peptides*, 1985, **6**, 161.
38 S. G. Farmer and R. M. Burch, in *Bradykinin Antagonists. Basic and Clinical Research*, ed. R. M. Burch, Marcel Dekker Inc., New York-Basel-Hong, Kong, 1991, pp. 1-31.
39 J. M. Stewart, *Biopolymers*, 1995, **37**, 43.
40 M. Śleszyńska, A. Kwiatkowska, D. Sobolewski, T. H. Wierzba, J. Katarzyńska, J. Zabrocki, L. Borovickowa, J. Slaninova and A. Prahl, *Acta Bicochim Pol.*, 2009, **56**, 641.
41 J. M. Stewart, L. Gera, W. Hanson and J. S. Zuzack, *Immunopharmacology*, 1996, **33**, 51.
42 J. Sejbal, J. R. Cann, J. M. Stewart, L. Gera and G. Kotovych, *J. Med. Chem.*, 1996, **39**, 1281.
43 S. S. Wang, *J. Am. Chem. Soc.*, 1973, **95**, 1328.
44 P. Holton, *Br. J. Pharmacol.*, 1948, **3**, 328.
45 B. Lammek, Y. X. Wang, I. Gavras and H. Gavras, *Peptides*, 1990, **11**, 1041.
46 B. Lammek, Y. X. Wang, I. Gavras and H. Gavras, *J. Pharm. Pharmacol.*, 1991, **43**, 887.
47 K. E. Korte, S. E. Skrabalak and Y. Xia, *J. Mater. Chem.*, 2008, **18**, 437.
48 A. Savitzky and M. J. E. Goly, *Anal. Chem.* 1964, **36**, 1627.
49 Y. Bi, H. Hu and G. Lu, *Chem. Commun.*, 2010, **46**, 598.
50 Y. Xiong, Y. Xie, C. Wu, J. Yang, Z. Li and F. Xu, *Adv. Mater.*, 2003, **15**, 405.
51 E. Proniewicz, D. Skołuba, I. Ignatjev, G. Niaura, D. Sobolewski, A. Prahl and L. M. Proniewicz, *J. Raman Spectrosc.*, 2013, **44**, 655.
52 E. Proniewicz, I. Ignatjev, G. Niaura, D. Sobolewski, A. Prahl and L.M. Proniewicz, *J. Raman Spectrosc.*, 2013, **44**, 1096.
53 D. Skołuba, D. Sobolewski, A. Prahl and E. Proniewicz, *Spectrosc-Int J.*, 2014, **2014**, 1.
54 J. W. Fox, R. J. Vavrek, A. T. Tu and J. M. Stewart, *Peptides,* 1982, **1**, 193.
55 Y. Hao and Y. Fang, *J. Nanopart. Res.*, 2007, **9**, 817.
56 L. A. Sanchez, R. L. Birke and J. R. Lombardi, *J. Phys. Chem.*, 1984, **88**, 1762.
57 M. T. Güllüoğlu, Y. Erdoğdu and S. Yurdakul, *J. Mol. Struct.*, 2007, **834-836**, 540.
58 T. Kupka, R.Wrzalik, G. Pasterna and K. Pasterny, *J. Mol. Struct.*, 2002, **616**, 17.
59 A. A. El-Azhary and R. H. Hilal, *Spectrochim. Acta, Part A* 1997, **53**, 1365.
60 J. J. Lopez, A. K. Shukla, C. Reinhart, H. Schwalbe, H. Michel and C. Glaubitz, *Angew. Chem. Int. Ed.*, 2008, **47**, 1668.
61 R. C. Mehrotra and R. Bohra, *Metal Carboxylates*, Academic Press, New York, 1983.
62 Zh. Nickolov, G. Georgiev, D Stoilova and I. Ivanov, *J. Molec. Struct.*, 1995, **354**, 119.
63 A. Kudelski, *Chem. Phys. Lett.*, 2006, **427**, 206.
64 A. Kudelski, *Vib. Spectrosc.*, 2006, **41**, 83.
65 C. Pardanaud, C. Martin, P. Roubin, G. Giacometti, C. Hopf, T. Schwarz-Selinger and W. Jacobs, *Diam. Relat. Mater.*, 2013, **34**, 100.

